Effect of Unmodified and Modified Nanocrystalline Cellulose Reinforced Polylactic Acid (PLA) Polymer Prepared by Solvent Casting Method

Morphology, mechanical and thermal properties

SITI NORBAYA KASA[1,2], MOHD FIRDAUS OMAR[2,3]*, MOHD MUSTAFA AL BAKRI ABDULLAH[3,4], ISMARUL NIZAM ISMAIL[2], SAM SUNG TING[3], SEBASTIAN CALIN VAC[5], PETRICA VIZUREANU[3,6]

[1] School of Materials Engineering, Universiti Malaysia Perlis, Kompleks Pengajian Jejawi 2, 02600 Arau, Perlis

[2] Advance Material Research Centre (AMREC), SIRIM BHD, Lot 34, Jalan Hi-Tech 2/3, Kulim Hi-Tech Park, Kedah, 09000 Kulim, Malaysia

[3] Centre of Excellence Geopolymer & Green Technology (CEGeoTech), School of Materials Engineering, Universiti Malaysia Perlis, Kompleks Pengajian Jejawi 2, 02600 Arau, Perlis

[4]Faculty of Engineering Technology (FETech), Universiti Malaysia Perlis (UniMAP), 01000, P.O.Box, D/A Pejabat Pos Besar, Kangar, Perlis, Malaysia

[5] University of Agricultural Sciences and Veterinary Medicine of Cluj Napoca, Faculty of Horticulture, 3-5 Manastur Str. , Cluj Napoca, 400372, Romania

[6]Gheorghe Asachi Technical University of Iasi, Faculty of Materials Science and Engineering, 41A D Mangeron Blvd., 700050, Iasi, Romania

The positive attributes of excellent biocompatibility and biodegradability of biocomposites with the addition of versatile nanocellulose from agriculture wastes have provided plenty opportunities for further development of functional biocomposite in various fields. Therefore, solvent casting was selected as a reinforcement method in order to produce biocomposite comprise of nanocrystalline cellulose and PLA polymer. Modification of nanocrystalline cellulose through acetylation reaction was conducted upon reinforcement to reduce its surface polarity and hidrophilicity. Biocomposite films prepared at various unmodified (uNC) and acetylated nanocrytalline cellulose (aNC) loading were exposed to morphological (FESEM), tensile test and thermal analysis (TGA). Reinforcement of aNC shows a better dispersion in PLA polymer due to the decreasing of surface polarity, thus increasing inter-facial interaction between both materials. This is proven by greater performance of biocomposite films in tensile strength, Young's modulus and thermal stability of aNC reinforced PLA as compared to uNC reinforced PLA. Overall, it can be concluded that these research findings can widen the scope of biocomposites research area and have significant implications for the commercial application of biomass products.

Keywords: acetylated nanocellulose, nanocellulose reinforced PLA, characterization and properties

Considerable research towards the development of new polymer material with low environmental impact has been risen in order to overcome the waste disposal problem cause by the massive usage of petroleum derivative polymer in plastic production (i.e. polyethylene, polypropylene and polystyrene). These petroleum-based plastics need 400-500 years to naturally degrade, therefore incineration is an alternative method applied for disposal purpose in most countries. However, this method creates harmful byproducts to environment such as increasing in carbon dioxide concentration and releasing of other toxic gas [1]. Due to the crucial waste disposal issue, aliphatic polyesters such as polylactic acid (PLA), polyhydroxy-butyrate-co-valerate (PHBV), polycaprolactone (PCA) and polyglycolic acid (PGA) have been developed and identified as the most suitable replacement material with high biodegradability properties and low production cost that synthesized from renewable resources such as corn, starch and sugar beet [2]. Among these bio-polymers, PLA have gained great attention because of its excellent commercial potential value like thermal properties, biocompatibility, and processability in most equipment. High demand of PLA in engineering plastic due to the wide range of applications (i.e. textiles, medical device, packaging material, automobile parts and films) have lowered the current PLA market price [3]. Unfortunately, there are certain weakness of PLA as food packaging due to its high brittleness, low heat resistance, low mechanical properties and poor barrier properties [4]. New phase of research proposes the reinforcement of nanomaterial into PLA polymer in order to enhance thermal, mechanical and barrier properties. Extensive research has been focused on the application of nanocrystalline cellulose as reinforcing material due to its special characteristic that qualify nanocrystalline cellulose as reinforcing material in polymer matrices; large specific surface area (several hundreds of $m^2 g^{-1}$), low density (about 1.566gcm^{-3}), high modulus of elasticity (approximately 150 GPa), bio-compatibility and biodegradability [5].

The two most popular reinforcement methods introduced by Jonoobi et al. [6] are solvent casting by using solvent as mixing medium and melt mixing by applying high temperature during processing. However, there are some challenge needs to be solved through both methods in order to achieve the uniform dispersion and avoid agglomeration of reinforcing material in polymer matrix. Besides that, melt mixing or melt compounding reinforcement method involves high temperature, which up to 200^oC during processing. Even though, this method is

* email: firdausomar@unimap.edu.my

claimed as a green process which means solvent free and economical. However, incompatibility and thermal stability still become the main issue due to the hydrophilic nature of nanomaterials especially nanocrystalline cellulose, which can cause an aggregation during the mixing with non-polar matrices due to the presence of hydroxyl groups that contribute to the formation of hydrogen bonding between nanomaterials [7].

To overcome this problem, modification reaction towards the surface of nanocrystalline cellulose can be implemented. There are three most popular modification reaction proposed by Abdulkhani et al. [2], that are silane treatment, acetylation reaction and TEMPO oxidation. Acetylation reaction or also known as a solvent exchange process involving the usage of acetic anhydride or acetic chloride as the acetylation reagent with the presence of sulfuric acid or perchloric acid as a catalyst [8]. This process involves the replacement of hydroxyl (–OH) groups at the end of cellulose structure by an acetyl (CH_3) groups to reduce the high polarity of nanocrystalline cellulose, thus increasing its hydrophilic behavior [9]. While, silane coupling is the treatment involving hydrolysis, condensation and bond formation phase for the purpose of improving the degree of cross linking of interface region. Formation of silanols occurs with the presence of moisture via hydrolysis of alkoxyl group. The process was continued by the reaction of silanols with the hydroxyl group of fibers to form stable covalent bonds to the cell wall that is chemisorbed onto the fiber surface. Based on Islam et al. [9], crosslink network was created due to the covalent bond between the matrix and filler. TEMPO oxidation also one of the famous modification methods which the main idea is to oxidize nanocrystalline cellulose by using 2,2,6,6 tetramethyl-1-piperidinyloy (TEMPO) as a catalyst with the presence of NaClO and NaBr at room temperature. During this process, hydroyl group (OH) located at carbon no 6 (C6) of nanocrystalline cellulose will be converted to carboxylate group. Higher amount of NaClO is required to get the highest number of carboxylic group attached at the surface of nanocrystalline cellulose [10]. However, this study focused on the modification through acetylation reaction and the reinforcement was conducted via solvent casting method. Performance of biocomposite film was investigated in terms of their morphological, mechanical and thermal properties.

Experimental part

Materials

Dried banana stem was used as raw material to synthesize nanocrystalline cellulose. Sodium hydroxide (NaOH), sodium chlorate ($NaClO_3$) and sulfuric acid (H_2SO_4 95.0 - 98.0 wt. %) were purchased from Sigma Aldrich. Polylactic acid (PLA) purchased from Repreper Tech Co. as polymer matrix used with the melting temperature at 175~220°C approximately and density is 124 g/cc. Chloroform was purchased from Fisher Scientific, UK for solvent casting process.

Pre-treatment of banana stem

Pre-treatment was conducted in order to remove lignin and hemicellulose in banana stem fibers. 2% of NaOH solution was used for lignin removal by stirring at 80°C for 4 hours and followed by washing with distill water during filtration. The process was repeated for three times. An equal solution of acetate buffer (27 g NaOH and 75 mL glacial acetic acid diluted to 1 L of distilled water) and sodium chlorate solution (1.7 weight % $NaClO_3$ in distilled water) with the ratio of 1:1 was prepared for cellulose bleaching treatment. Cellulose-acetate buffer solution was stirred at 300 rpm for 4 h at 80°C. Cellulose fibers were filtered and neutralized to *p*H 7 followed by drying in circulating oven at 40°C for overnight.

Preparation of nanocrystalline cellulose

Pre-treated banana stem fibers were synthesized by 54% H_2SO_4 solution under strong mechanical stirring at 50°C for 1 hour. Cellulose whisker was then diluted 10 times fold of distill water immediately to inhibit the reaction and followed by centrifugation at 10,000 rpm, 10 min per cycle. The acidic cellulose precipitate was dialyzed with distill water until reach *p*H 7. The suspension was then ultrasonicated at 4 Hz for 10 min to disperse the nanocrystalline cellulose (uNC) and stored in refrigerator at 5°C for further used.

Acetylation reaction of nanocrystalline cellulose (aNC)

uNC was stirred in 25% of acetic acid and a few drops of sulfuric acid for 30 min at 70°C to activate its surface and followed by centrifugation at the speed of 10,000 rpm for 10 min. 100 mL Acetic acid was added into the uNC sediment and stir at 100°C for 4 h and the excess acetic acid was removed by centrifugation. Acetylated nanocrystalline cellulose (aNC) was then soaked and stir in 100 mL of acetone:ethanol (2:1) mixture for 1 h to remove excess water and followed by drying in circulating oven for 12 h. aNC powder was collected and stored in dry cabinet.

Preparation of biocomposite film

Neat PLA film was prepared by stirring 5g of PLA pallet into 100 mL chloroform for 1 h at 50°C and cast the solution into a petri dish, chloroform was allowed to slowly evaporate at room temperature for overnight. Untreated nanocrytalline cellulose reinforced PLA (uNC-PLA) film was prepared at four different formulations as shown in table 1. uNC powder was dissolved in chloroform by stirring at 50°C for two hours and followed by ultrasonication for 15 min. PLA solution was prepared separately by dissolving it in chloroform at 50°C for h . uNC and PLA solution were mixed by stirring at 50°C for 3 h and followed by ultrasonication for 30 min. The mixtures were then poured into a petri dish and let the chloroform slowly evaporated at room temperature for overnight. The smilar preparation method was applied for aNC-PLA and the formulation was shown in table 1.

Morphological analysis

Morphology was observed by using field emission scanning electron microscope (FESEM - Hitachi UHR FESEM SU9000) with an accelerating voltage of 5kv and in SE signal after been coated with silver particles by vacuum sputter coater at a low deposition rate.

Identification	uNC (g)	PLA (g)
100% PLA	0.0	10.0
1wt. % uNC-PLA	0.1	9.9
3wt. % uNC-PLA	0.3	9.7
5wt. % uNC-PLA	0.5	9.5
7wt. % uNC-PLA	0.7	9.3

Table 1
FORMULATION OF uNC AND aNC REINFORCED PLA BIOCOMPOSITE FILMS

Crystallinity analysis

Crystallinity was obtained by X-ray difractometer (XRD - Bruker AXS D8 Advance) with Cu-kα radiation source ($\lambda = 1.54\text{Å}$) at an accelerating voltage of 40kV. The diffractogram was recorded in the $\varphi = 2\theta$ angle ranged from 10- 90° with a step interval size of 0.04 and data was collected at scan rate of 1°/min. The crystallinity index was calculated from the heights of the 002 peak (I_{002}, $2\theta = 22.6^{o}$) and the intensity minimum between the 002 and $\bar{1}11$ peaks (I_{am}, $2\theta = 18^{o}$) using the Segal method (eq.1). Where I_{002} is an intensification of the 002 reflectance and *IAM* is the minimum intensity at $2\theta = 18$ °.

$$\text{Crystalline index (CrI):} \left(\frac{I002 - I_{AM}}{I002} \right) \text{X } 100 \qquad (1)$$

Spectroscopic analysis

Spectroscopic analysis was examined by using Fourier transform infrared (FTIR - Perkin Elmer). Spectra were taken at a resolution of 4 $cm^{-1,}$ with a total of 16 scans for each sample and the experiment was carried out at spectrum range of 4000 - 600 cm^{-1}.

Tensile analysis

Mechanical properties were measured by using the ultimate testing machine (UTM - Tinius Olsen H5KS) at room temperature, 25°C. Average thickness and width were recorded using a micrometer caliper prior to the test. The machine direction (MD) with a crosshead speed of 5.0 mm/min was set. Tensile strength (TS) was determined by dividing the maximum load on the film before failure by the cross-sectional area of the initial specimen. Elastic modulus (EM) was calculated by dividing the tensile stress by the extensional strain as shown in eq. 2 (Young's modulus) and elongation at break (E) was defined the percentage change in the length of the specimen compared to the original length between grip.

$$E \equiv \frac{\text{tensile stress}}{\text{extension strain}} = \frac{\sigma}{\varepsilon} = \frac{F/A_0}{\Delta L/L_0} = \frac{FL_0}{A_0/\Delta L} \qquad (2)$$

where:

E is the Young's modulus

F is the force exerted on an object under tension

A_0 is the original cross-sectional area through which the force is applied

ΔL is the amount by which the length of the object changes

L_0 is the original length of the object

TGA analysis

Thermal properties were measured by using a thermogravimetric analyzer (TGA) at a running temperature 30 to 700°C with the programmed heating rate 10°C/min and sample mass between 5 to 10 mg on alumina pans.

Results and discussions

Morphology analysis

Figure 1(a) shows the image and FESEM micrograph of unmodified nanocrystalline cellulose (uNC). After the drying process, uNC can be visually observed in thin film form because of an agglomeration of uNC during the evaporation of water. This is verified by the FESEM image which shows the smooth surface rigid rod-like shape of uNC with mostly agglomerated. This phenomenon occurs because of its hydrophilicity behavior due to the presence of hydrogen (H^+) and hydroxyl (OH^-) groups at the end of the uNC chemical structure which tend to form inter-chain and intra-chain hydrogen bonding as illustrated in figure 2.

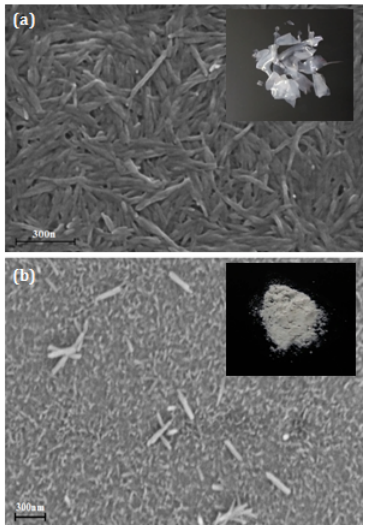

Fig.1. Physical appearance and FESEM micrograph of (a) uNC and (b) aNC

Abraham et al. [11] mentioned that due to the nano size of cellulose, plenty of hydroxyl groups are allowed to attach at each of uNC interfaces, therefore increasing its hydrophilic properties. From this study, the average dimension of uNC measured are 287.0 ± 56.4 nm in length and 26.6 ± 4.8 nm in diameter. While, calculated aspect ratio *(L/d)* is 10.87 approximately.

Surface modification via acetylation reaction was carried out for the aim to decrease the uNC surface polarity from hydrophilic to hydrophobic properties. The heterogeneous acetylation reaction was conducted without applying any other solvent, but only acetic acid as an acetyl source and sulfuric acid as a catalyst. Interestingly, acetylation reaction has definitely changed the physical appearance of uNC as shown in figure 1. Acetylated nanocrystalline cellulose (aNC) can visually

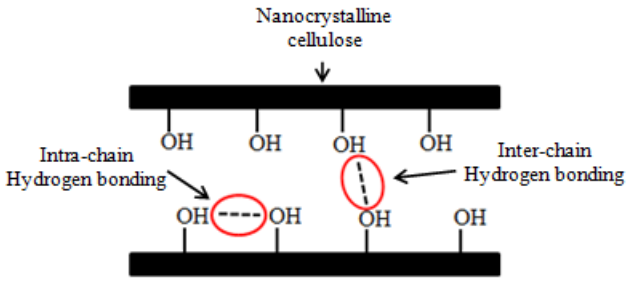

Fig.2. Chemical structure of Inter-chain and intra-chain bonding of uNC

observe in fine powder form after the drying process. The FESEM micrograph of aNC also clearly shows the formation of single and well dispersed of nanocrystals. Furthermore, Islam et al. [9] described that acetylation reaction has definitely converted the properties of uNC from hydrophilic to hydrophobic behavior due to the substitution of hydroxyl (OH^-) groups by an acetyl (CH_3CO) groups at the end of nanocrystalline cellulose structure as illustrated in figure 3.

Chemical composition analysis

Chemical composition of nanocrystalline cellulose before and after acetylation reaction was observed using FTIR and the spectra was shown in figure 4. The uNC spectra in fi8gure 4(a) that gives a broader peak near 3350cm^{-1} is correspond to the hydroxyl (-OH) groups exist on uNC molecules. Absorption peak near 2924cm^{-1} is due to the aliphatic saturated C-H stretching vibration in

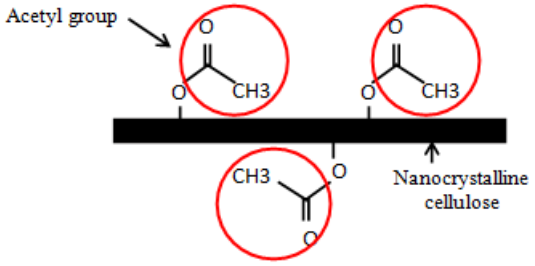

Fig. 3. Chemical structure of acetylated nanocrystalline cellulose (aNC)

cellulose and hemicellulose [12]. Peak around 1691cm^{-1} is an absorbed water in uNC molecules [6]. Peak at 1437cm^{-1} represent the –CH_2- bending and sharp peak at 1339cm^{-1} indicates the –C-H asymmetric deformation, while peak near 1057cm^{-1} is the –C-O-C- pyranose ring skeletal. Based on Elanthikkal et al. [13], increasing in intensity of band 1057cm^{-1} indicates the increasing in cellulose content.

As shown in figure 4 (b), three new absorption band appears for aNC sample due to the existing of acetyl groups on its surface. These three main peaks were found near 1731cm^{-1}, 1373cm^{-1} and 1235cm^{-1} which attributed to the C=O stretching of the carbonyl group, CH_3 in-plane bending and C-O stretching of acetyl groups. Similar absorption pattern also reported by Jonoobi et al. [6] in his study. According to Yan et al. [13], the appearance of these three main peaks identifies that the acetylation reaction has been successfully covert the unmodified nanocrystalline cellulose to acetylated nanocrystalline cellulose.

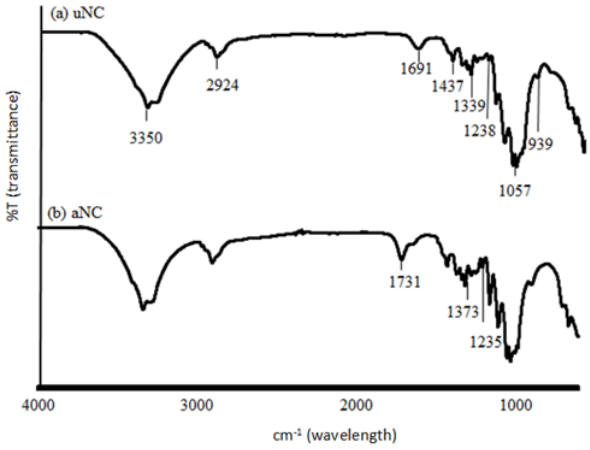

Fig. 4. FTIR spectra of (1) unmodified nanocrystalline cellulose and (b) acetylated nanocrystalline cellulose

Crystallinity analysis

XRD analysis was used in order to determine the effect of acetylation reaction towards the crystallinity index of nanocrystalline cellulose, and the diffraction pattern was given in figure 5. As mentioned by Santos et al. [15], diffractogram which exhibit an amorphous broad hump and sharp crystalline peak is acknowledged that both nanomaterial is in semi-crystalline form. The diffractogram of uNC showed in figure 5(a) was exhibited by type I cellulose with an amorphous broad hump and sharp crystalline peak of cellulose. This is verified by the presence

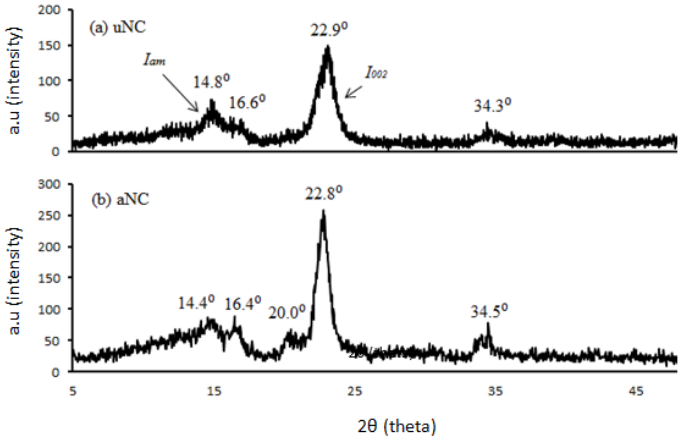

Fig. 5. XRD patterns of (a) uNC and (b) aNC

of peak at 2θ=14.8° (plane 101), 2θ=16.6° (plane 10î), a sharp peak at 2θ=22.9° (plane 002) and small broad peak at 2θ=34.3° (plane 004) [15]. Almost similar major reflection peak appear after an acetylation reaction at 2θ=14.4°, 2θ=16.4°, 2θ=22.8° and 2θ=34.5°.This is similar with the result reported by Jonoobi et al. [6] which highlighted that there is no changes in main diffraction pattern even after experience the chemical modification. Except for the appearance of new small broad hump around 2θ=20.0° for aNC sample attributes to the presence of grafted aliphatic chains which considering the acetylation reaction has partially converted the cellulose type I into cellulose type II [14-16]. The Crystallinity index was calculated using Segal method and intensity of both samples has been summarized in table 2. From the data, we can pre-conclude that acetylation reaction has increased the crystallinity index of nanocrystalline cellulose from 51.04% up to 67.32%. This may be due to the dispersion of nanocrystalline cellulose after being modified. Dai, Fans & Collins [18] stated that the great distribution and inter-facial properties of nanocrystals determines the final performance of biocomposites.

Mechanical analysis of composites

It is believed that the reinforcement of nanomaterials into the polymer matrix gives high impact towards the biocomposites mechanical properties. Therefore, tensile properties of biocomposite films were tested and the results were portrayed in figure 6. The tensile strength of the neat

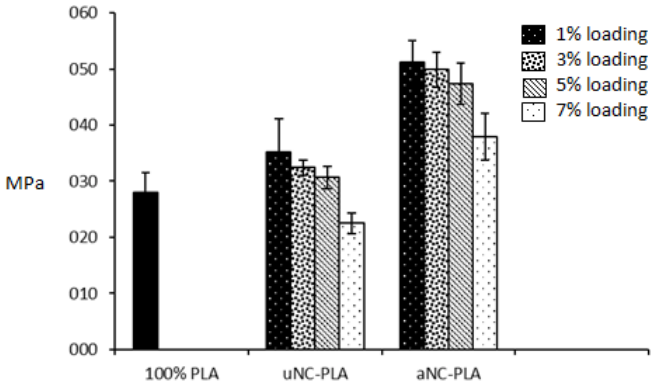

Fig.6. Tensile strength of uNC-PLA and aNC-PLA at different loading

Sample	Intensity (a.u)		Crystallinity index (%)
	I_{am}	I_{002}	
uNC	70.98	144.97	51.04
aNC	83.01	254.00	67.32

Table 2
INTENSITY AND CRYSTALLINITY INDEX OF uNC AND aNC

PLA film is 28.0 MPa. While, tensile strength of uNC reinforced PLA shows the highest value at 1wt.% uNC loading with 25.72% increment. However, the tensile strength value after 3wt. % and 5wt. % uNC loading was gradually decreased to 15.76% and 9.47%. Meanwhile, at 7wt. % uNC loading has reduced film tensile strength about 19.66% lower than the neat PLA film. Yan et al. [16] explained that the agglomeration occurs at high uNC loading would weaken the intermolecular interaction between reinforcing material and polymer matrix. As described by Abdulkhani et al. [2], the excess amount of reinforcing material may increase the brittleness of thin film due to the agglomeration of nanomaterials in the film and show the reverse effect on the mechanical properties of biocomposite.

On the other hand, reinforcement of 1wt. % aNC into PLA has greatly improved the film strength up to 82.7% as compared to 1. % uNC loading (25.72%). This result has proved that the great dispersion of nanocrystalline cellulose has increased the compatibility between polymer matrix. Moreover, increasing in crystallinity of nancrystalline cellulose after an acetylation reaction has transformed the nanocrystalline cellulose to become a great reinforcing material [2]. Besides, at 3wt. %, 5wt. % and 7wt. % aNC loading were also gradually decrease in tensile strength to 78.2, 69.0 and 35.6%. However, aNC-PLA film still gives higher tensile strength value than uNC-PLA film even though at higher loading. Reducing in hydrophilicity of reinforcing material has increased the solubility of aNC in the solvent during the mixing with PLA and reduce the potential of agglomeration during the casting process. This will increase the inter-facial interaction of both materials, hence resulted in high tensile strength of the film produced. According to Dufresne et al. [19], adhesion and compatibility, volume fraction, aspect ratio, orientation, crystalinity and stress transfer efficiency of reinforcing material gives great influence towards the overall performance of bio-composites.

The reinforcement of uNC and aNC into PLA also expected to improve Young's modulus that measures the stiffness of the membrane. The value was obtained by the calculation from stress-strain curves and the result was represented in figure 7. As can be seen in the chart, Young's modulus also shows the same trend as tensile modulus which gives the highest value for 1wt. % loading and lowest value for 7wt. % loading. Young's modulus of neat PLA film is 8.95 GPa. As predicted, the reinforcement of 1wt. % uNC has increased 33.9% of Young's modulus, whilst reinforcement of 1wt. % aNC has given large increment in Young's modulus which is up to 118.7%. Lalia et al. (2014) stated that the improvement in the Young's modulus after the reinforcement is due to the stiffness properties of uNC and aNC that has been dispersed in PLA polymer. However, after being reinforced with 3wt. %, 5wt. % and 7wt. % loading, Young's modulus gradually decreased either for the untreated or acetylated nanocrystalline cellulose. Similar finding was reported by Lalia et al. [20] where the authors mentioned that the agglomeration of reinforcing material has increased the inhomogeneity of biocomposite and act as sites of stress concentration, decreasing the tensile strength and Young's modulus of the film. For better understanding of the result discussed, an illustration of the dispersion and inter-facial interaction of reinforcing material in PLA polymer was proposed in figure 8.

Thermal degradation analysis of biocomposite

Thermal performance of PLA films incorporated with uNC and aNC as reinforcing material at various loading

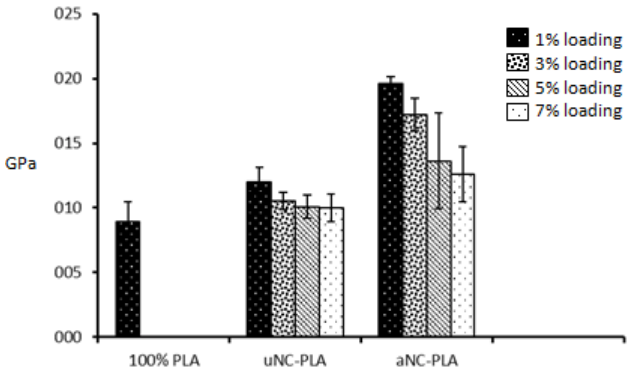

Fig.7. Young's modulus of uNC-PLA and aNC-PLA at different loading

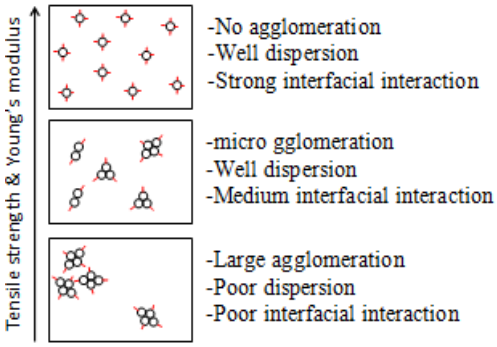

Fig.8. Schematic diagram of reinforcing material dispersion and inter-facial Interaction in PLA polymer

proportions was examined using TGA. As seen in figure 9 and figure 10, all samples show the initial weight loss around 80 -140 °C that could be due to the evaporation of bounded moisture at the surface of the bio-composites film. According to Lee et al. [21], this caused by an evaporation of physically weak and chemically strong bound water. Thermal degradation of pure PLA is approximately occurs at 291°C and completes around 376 °C. The highest shifted degradation temperature is around 309°C with the incorporation of 1wt. % of uNC. However, there is no significant influence in thermal degradation even at higher uNC loading. A study by Cho & Park [22] also stated that no significant effect on thermal stability at low nanocrystalline cellulose loading. However, PLA incorporate with aNC gives higher increment in thermal degradation temperature and considerably slows down the degradation rate. Degradation temperature of bio-composite film has increased to 324, 320, 316 and 318°C as the reinforcing material increase from 1wt.% to 7wt.%. The first stage of major degradation temperature was observed around 310 - 387°C for all samples and this indicates that a large volatilization of polymer take part

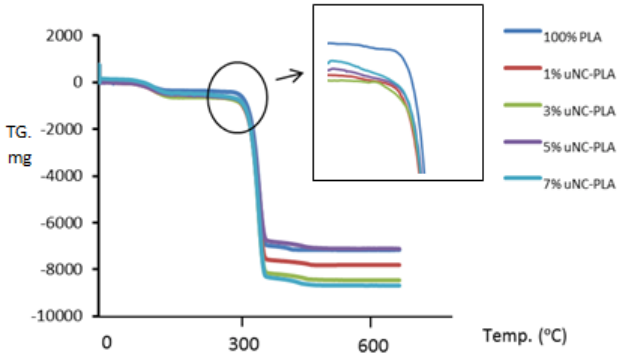

Fig. 9. TGA curves of PLA and uNC-PLA at different loading

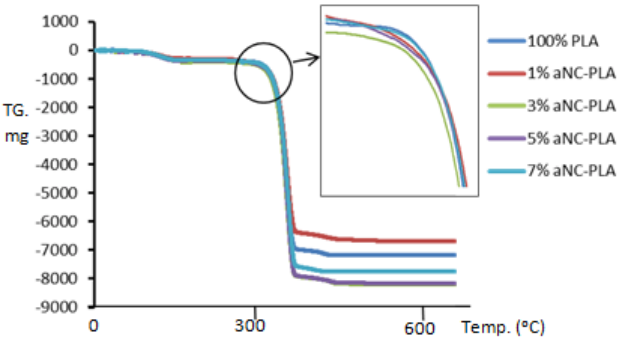

Fig.10. TGA curves of PLA and aNC-PLA at different loading

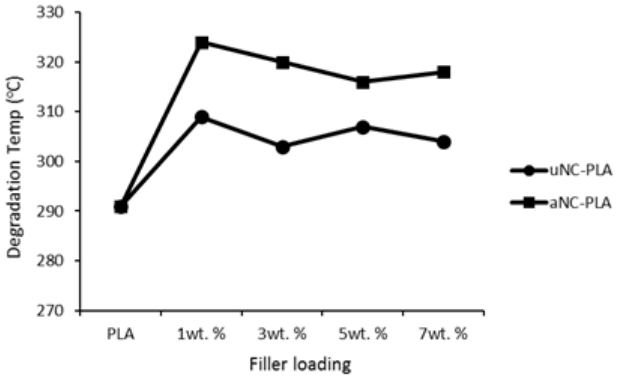

Fig. 11. Degradation temperature of uNC-PLA and aNC-PLA

due to the thermal scission of the polymer backbone and pyrolysis of nanocellulose fiber. Second stage of degradation occurs around 420 - 460°C for all samples due to the decomposition of carbonaceous matter as pointed by Panaitescu et al. [23]. This result proved that the great dispersion of aNC in polymer matrix influence the degradation temperature of bio-composites film and the overall view of the result was summarized in figure 11.

Morphological analysis of biocomposite

The fracture surface of biocomposites was evaluated by using FESEM to study the influence of nanomaterial introduction into PLA polymer at different loading rate. As seen in figure 12 (a), uniform dispersion of aNC in PLA polymer at 1wt. % loading was observed. Even though uniform dispersion was achieved, the tensile strength of 1% uNC-PLA exhibit smaller increment (25.2%) as compared to reinforcement of 1wt.% of aNC into PLA polymer (82.7%). This is due to the hydrophilic properties of uNC having less interaction with the hydrophobic polymer, therefore, affects the mechanical and thermal performance of films. Figure 12 (b), (c) and (d) indicates the poor distribution of reinforcing material due to the increasing of uNC agglomerated size as the amount of reinforcing material increase from 5wt. % up to 7wt. %. This finding is consistent with the work reported by Jonoobi et al. [24], where the authors mentioned that there is no significant difference in terms of distribution for addition of unmodified nanocrystalline cellulose, while rougher surface and small agglomerates were also found at higher loading [25, 26]. Meanwhile, aNC reinforced PLA polymer demonstrates more uniform distribution for 1wt. %, 3wt. % and 5wt. % of aNC loading as shown in figure 12 (e), (f) and (g). This indicates that the acetylation process successfully increases the hydrophobicity and distribution of nanocrystalline cellulose in polymer matrix. Previous study by Jonoobi et al. [6] mentioned that agglomeration occurs at early 5% for aNC reinforcement via twin screw extrusion method. This result verified that reinforcement via solvent casting achieved better dispersion of reinforcing material. However, tensile strength at 3wt. % and 5wt. % aNC loading decreased about 4.5 and 9.2%, respectively, due to the increasing of aNC agglomeration size, thus reducing the surface area interaction between both materials. Furthermore, larger agglomeration and poor distribution of filler was obviously appears at 7wt. % aNC loading as can be seen in figure12(h). This may pre-conclude that the decreasing in surface polarity and lower amount of reinforcing material leads to better dispersion and inter-facial interaction of nanocrystalline cellulose in hydrophobic polymer matrix.

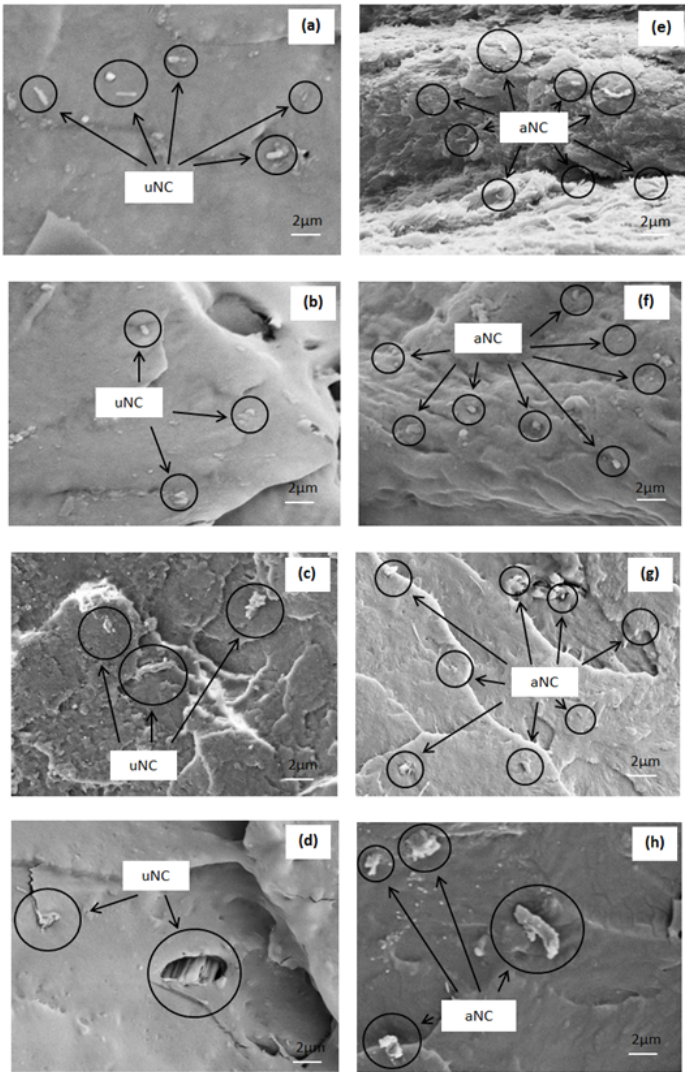

Fig.12. Fracture surface of nanocrystalline cellulose reinforced PLA : (a) 1% uNC-PLA, (b) 3% uNC-PLA, (c) 5% uNC-PLA, (d) 7% uNC-PLA, (e) 1% aNC-PLA, (f) 3% aNC-PLA, (g) 5% aNC-PLA and (h) 7% aNC-PLA

Conclusions

This study demonstrates that the acetylation reaction of nanocrystalline cellulose was successfully conducted based on the morphological study, chemical composition and crystallinity study. Reinforcement of untreated and acetylated nanocrystalline cellulose into PLA polymer was effectively carried out via solvent casting method and the effect of reinforcement towards morphology, mechanical and thermal properties were compared. Microscopic study of biocomposite indicates that the acetylated nano-crystalline cellulose gives a better dispersion in polymer matrix. Furthermore, both reinforcing materials give positive

effect towards tensile and Young's modulus. However, acetylated nanocrystalline cellulose exhibit higher improvement in both parameters tested due to the great dispersion and inter-facial interaction between polymer matrix. Besides, thermal stability also shows improvement after addition of acetylated nanocrystalline cellulose, while no significant effect after addition of untreated nanocrystalline cellulose. This result indicates that the acetylation reaction has improved the capability of nanocrystalline cellulose to be applied as reinforcing material for PLA polymer.use.

Acknowledgement: The author would like to acknowledge Universiti Malaysia Perlis (UniMAP) (Grant no.: 9003-00390, 9007-00067, 9017-00014, 9007-00130) and Advance Material Research Centre (AMREC), SIRIM BHD for sponsoring and providing financial assistance for this research work.

References

1.MODI, S., KOELLING, K., VODOVOTZ, Y., European Polymer Journal, **49**, no 11, 2013, p. 3681.
2.ABDULKHANI, A., HOSSEINZADEH, J., ASHORI, A., DADASHI, S., & TAKZARE, Z., Polymer Testing, **35**, 2014, p.73.
3.AWAL, A., RANA, M., SAIN, M., Mechanics of Materials, **80**, 2014, p. 87.
4.ARRIETA, M. P., FORTUNATI, E., DOMINICI, F., RAYON, E., LOPEZ, J., KENNY, J. M., Carbohydrate Polymers, **107**, no 1, 2014, p.16.
5.EICHHORN, S. J., DUFRESNE, A., ARANGUREN, M., MARCOVICH, N. E., CAPADONA, J. R., ROWAN, S. J., PEIJS, T., Journal of Materials Science, **45,** 2010, p.1
6.JONOOBI, M., MATHEW, A. P., ABDI, M. M., MAKINEJAD, M. D., OKSMAN, K., Journal of Polymers and the Environment, **20**, no 4, 2012, p.991.
7.DUFRESNE, A. , Materials Today, **16**, no 6, 2013, p. 220.
8.GRANSTRÖM, M., & KILPELAINEN, P. I., Department of Chemistry, 2009, p.1-120
9.ISLAM, M. T., ALAM, M. M., ZOCCOLA, M., International Journal of Innovative Research in Science, Engineering and Technology, **2**, no 10, 2013, p.5444.
10.MISSOUM, K., MARTOÏA, F., BELGACEM, MOHAMED, N. B., JULIEN, B., Industrial Crops and Products, 48, 2013, p.98
11.ABRAHAM, E., THOMAS, M. S., JOHN, C., POTHEN, L. A., SHOSEYOV, O., & THOMAS, S., Industrial Crops and Products, **51**, 2013, p.415.
12.FAN, J. S., LI, Y. H., Carbohydrate Polymers, **88**, no 4, 2010, p.1184.
13.ELANTHIKKAL, S., GOPALAKRISHNAPANICKER, U., VARGHESE, S., & GUTHRIE, J. T., Carbohydrate Polymers, **80**, no 3, 2010, p.852.
14.YAN, M., LI, S., ZHANG, M., LI, C., DONG, F., LI, W., BioResources, **8**, no 4, 2013, p.6330.
15.POPESCU, V., SANDU, I.C.A., POPESCU, G., Rev. Chim. (Bucharest), **67**, no. 10, 2016, p. 1994.
16.POPESCU, V., SANDU, I.G., VASLUIANU, E., SANDU, I., MANEA, L.R., CAMPAGNE, C., Rev. Chim. (Bucharest), **65**, no. 12, 2014, po. 1439.
17.SANTOS, R. M. DOS, FLAUZINO NETO, W. P., SILVÉRIO, H. A., MARTINS, D. F., DANTAS, N. O., PASQUINI, D., Industrial Crops and Products, **50**, 2013, p.707
18.DAI, D., FAN, M., COLLINS, P., Industrial Crops and Products, **44**, 2013, p.192–199.
19.DUFRESNE, A., DUPEYRE, D.,PAILLET, M., Journal of Applied Polymer Science , **87**, 2002, p. 1302-1315.
20.LALIA, B. S., GUILLEN, E., ARAFAT, H. A., HASHAIKEH, R., Desalination, **332**, no 1, 2014, p.134.
21.LEE, S. Y., MOHAN, D. J., KANG, I. A., DOH, G. H., LEE, S., HAN, S. O., Fibers and Polymers, **10**, no 1, 2009, p.77.
22.CHO, M. J., PARK, B. D., Journal of Industrial and Engineering Chemistry, **17**, no 1, 2011, p.36.
23.PANAITESCU, D. M., FRONE, A. N., GHIUREA, M., SPATARU, C. I., RADOVICI, C., IORGA, M. D., Advances in Composites Materials - Ecodesign and Analysis, 5, 2010, p.103.
24.JONOOBI, M., HARUN, J., MATHEW, A. P., & OKSMAN, K., Composites Science and Technology, **70**, no 12, 2010, p.1742
25. SANDU, A.V., BEJINARIU, C., NEMTOI, G., SANDU, I.G., VIZUREANU, P., IONITA, I., BACIU, C., Revista de Chimie, 64, no. 8, 2013, p. 825.
26. MOGA, I.C., PRICOP, F., IORDANESCU, M., SCARLAT, R., DOROGAN, A., Industria Textila, 64, no. 4, 2013, p. 222.

Manuscript received: 8.12.2016